PROCEEDINGS of
CHEF 2013

The Calorimeter of the *Fermi* Large Area Telescope

Carmelo Sgrò*
INFN-Pisa, Largo B. Pontecorvo, 3 - 56127 Pisa, Italy
E-mail: carmelo.sgro@pi.infn.it

on behalf of the *Fermi* LAT collaboration

The Large Area Telescope (LAT) is the main instrument on board of the *Fermi* mission. It is pair-conversion telescope designed to detect gamma rays from 20 MeV to more than 300 GeV. It is composed of 16 identical towers (tracker and calorimeter), covered by an anti-coincidence detector to reject charged particles. The LAT calorimeter is an hodoscopic array of CsI(Tl) crystals, arranged in 8 alternating orthogonal layers, with a thickness total of 8.6 radiation lengths. Each crystal is readout at both ends with PIN photodiodes to provide energy and position information. This configuration allows a three-dimensional imaging of the electromagnetic shower in order to improve energy reconstruction and background rejection. In this talk we will review the design and performance of the LAT and some of its scientific results. We will focus on the role of the calorimeter and show some recent development on the reconstruction, which will enhance the LAT performance for operations in the upcoming years.

Calorimetry for High Energy Frontiers - CHEF 2013,
April 22-25, 2013
Paris, France

*Speaker.

1. Introduction

The *Fermi* [1] observatory was launched in 2008 in an almost circular orbit at at 565 km altitude. Its main instrument is the Large Area Telescope (LAT), designed to explore the gamma-ray sky from 20 MeV to more than 300 GeV.

With about 5 years of flight data and its uniform coverage of the sky, the LAT allowed the first high statistics observations of gamma-ray sources of known classes as well as a discovery of new emitters [2]. The LAT allowed also a detailed study of the diffuse gamma-ray emission, which constitutes roughly 90% of the LAT photons, and constrains cosmic-ray production and propagation in our own Galaxy [3]. Stringent upper limit has been published on indirect Dark Matter search [4, 5], whitch is another important scientific goals of the experiment. Together with photons, the LAT proved to be able to detect cosmic-ray electrons and positrons, measure their spectra [6] and search for anisotropy in their incoming direction [7] .

2. The LAT design

The LAT is composed of high-energy physics detectors with the purpose of identify and reconstruct electromagnetic showers deriving from high-energy photon interactions. In this way we can measure the time, incoming direction and energy of gamma rays. The core of the instrument is a tracker-converter subsystem (TKR) made of silicon strip detector planes interleaved by tungsten foils to enhance photon interaction's probability, thus increasing the effective area of the telescope. The information from the tracker is used to reconstruct the electron-positron pair and measure the gamma-ray direction. An electromagnetic calorimeter (CAL), the main topic of this work, is placed below the tracker to absorb part of the shower energy. Its main purpose is to measure gamma-ray energy by imaging the development of the shower. The LAT design is modular (figure 1), the building block is a "tower" module that includes a TKR module followed by a CAL module. A 4×4 array of towers are kept together by an aluminum grid (the main mechanical structure). An anti-coincidence detector (ACD), made of plastic scintillator tiles, is placed around the tracker and provide a veto signal used to separate neutral from charged particle.

Operations in orbit impose very stringent limits on size, mass and power budget. Given the science requirement, the LAT and its subsystems have been designed as the best compromise between conflicting needs. The LAT is a discovery mission conceived to survey the highly unexplored gamma-ray sky where interesting phenomena can suddenly happen in any direction. Therefore all-sky monitoring capability is fundamental, in particular large area and field of view as well as small dead time. The typical gamma-ray sources have spectra that, to the first approximation, follow a power-law behaviour with index close to -2. For this kind of spectra only a moderate energy resolution is required, but a large collecting area is mandatory to be able to have a reasonable statistics at high energy. On the other hand, gamma-ray sources may have spectral features (breaks, cutoff or line search) that need to be measured precisely. and we can benefit from a good energy resolution.

Strong constraints are given by the launcher available for the mission. The Delta II used for *Fermi* permits a lateral size $\sim 1.8 \times 1.8$ m^2 and mass budget of about 3000 kg for the instrument ($\sim$ 1400 kg for the CAL, which, indirectly, sets the total depth). The total power budget comes

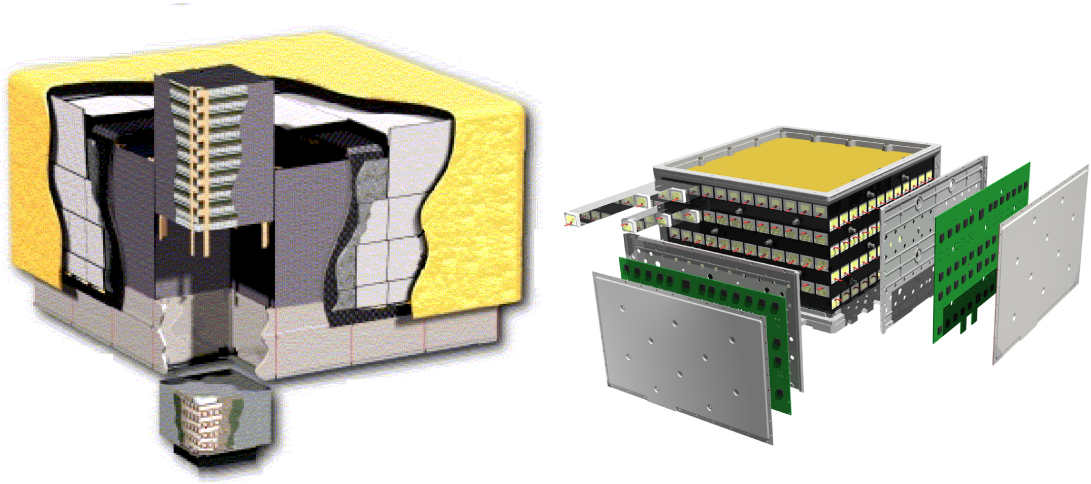

Figure 1: (*left*) Schematic diagram of the LAT. (*right*) Exploded view of a calorimeter module showing the hodoscopic 12×8 array of CsI(Tl) detectors in the carbon fiber structure. Two of four readout electronics circuit cards are shown in green.

from the solar panels and is of 650 W for the LAT and just ~ 60 W for the CAL. The details on the design and technology choices are described in [8].

3. The calorimeter

The calorimeter subsystem is composed of 16 modules, one per tower. Each module is composed of CsI(Tl) crystals bars arranged horizontally in 8 alternating orthogonal layers of 12 crystals each, as shown in figure 1. The crystal dimensions are $27 \times 20 \times 326$ mm^3, the vertical size is slightly more that one radiation length and the lateral size is slightly less that one Moliere radius. The crystals are inserted in a carbon fiber cell structure surrounded by alluminum closeouts. The scintillation light is readout by PIN photodiodes glued at both ends of the crystals and the front-end electronic boards are on the 4 lateral sides of the module.

With this geometry and by exploiting the light asymmetry from the two crystal ends, we can have a full three-dimensional reconstruction of the showers developing inside the CAL. This is very important since the CAL total depth is only 8.6 radiation lengths (with 1.5 added by the TKR on top) and the shower shape allows to correct for the leakage and provide quantities, like the lateral size, useful for hadronic background rejection. Moreover we can reconstruct the shower axis that can be used to select good quality events (exploiting the match with the TKR direction) and adds some imaging capability to the CAL alone.

The readout electronics is designed to have a dynamic range of a few times 10^5, a modest power consumption and minimal processing deadtime. Two PIN photodiodes are mounted in each crystal end, a small one for high energies and a big one for low energy. The signal from these devices is readout by custom ASICs, one per crystal end, featuring the analog amplification chain and two trigger signals. After a pre-amplifier stage, the signal from the two diodes is split to a fast shaping amplifier (~ 0.5 μs peaking time) for trigger discrimination and a slow shaping amplifier

(~ 3.5 μs peaking time) for spectroscopy. The trigger threshold are set to provide a low-energy trigger ($\sim$ 100 MeV per crystal) and a high-energy trigger ($\sim$ 1 GeV per crystal) in nominal flight operation. The output of each slow shaper is split into two track-and-hold stages with gain $\times 1$ and $\times 8$. Therefore four gain ranges are provided by each crystal end, to be able to measure from a few MeV up to $\sim$ 100 GeV. The reader should refer to [9] for further details on CAL design and construction.

The CAL functionality and performance are continuously monitored during nominal data taking. After 5 years in orbit no major failures have been observed. The calibration constants are regularly monitored and updated if necessary. We use periodic triggers, with a rate of 2 Hz, for pedestal monitoring, while charged cosmic rays, protons and heavy ions, are used to calibrate the energy scale of the lowest energy gain and the overlapping region between consecutive gain ranges. To correct electronics non linearities we use charge injection data from dedicated runs collected periodically. The light asymmetry inside each crystal is calibrated using non-interacting heavy nuclei and exploiting the tracker direction as reference. The radiation damage on CsI(Tl) crystals on orbit induces a decrease of the scintillation efficiency by $\sim 1\%$ per year, as expected from the pre-flight study. For more information on calibration procedure and study, we refer the reader to [10] and [11].

4. Event reconstruction in the CAL

The raw data from all the LAT subsystems are processed to reconstruct and select of good photon candidate. For a complete overview of reconstruction process and how the 3 subsystems are combined together, the reader should refer to [8].

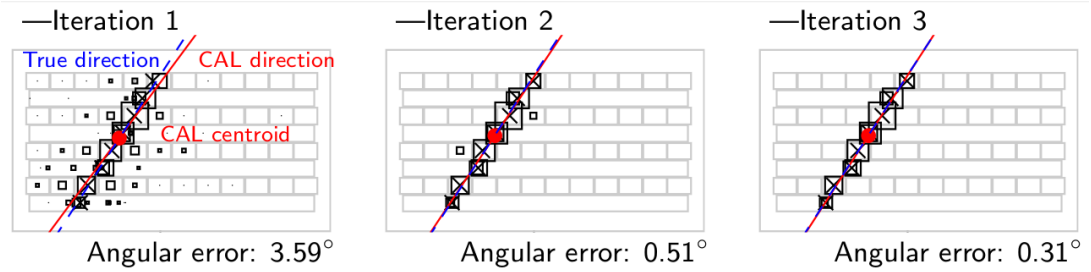

Figure 2: Example of iterative moment analysis with the LAT calorimeter. The shower axis (red continuos line) is evaluated as the principal axis of the energy deposition distribution. The true direction (blue dashed line) is progressively better estimated after each step.

For the CAL, after applying the calibration constants to convert the raw data to physical units, we begin with a shower shape analysis. First the energy centroid is evaluated, than the shower longitudinal axis (that corresponds to particle direction) is determined through a three-dimensional moments analysis in which the inertia tensor (with energy in place of of mass) is diagonalized. This is actually an iterative process, in which the hits far from the axis are progressively discarded. Figure 2 shows an example of these steps with a simulated event. It is possible to see how keeping only the core of the shower improves the final angular resolution of the CAL alone. The moment

analysis algorithm provides also eigenvalues that are useful to evaluate shower shape parameters and identify electromagnetic showers.

Two different algorithms are used for energy measurement, designed respectively for low and high energy. We found that this is the scheme that optimizes the performance in the entire energy range of the LAT. In fact, the CAL absorbs only part of the photon energy, but the energy loss mechanisms are different at low and high energy. As an example, photons below roughly 1 GeV lose a significant fraction of their energy in the TKR, while as the photon energy increases the leakage from the back of the CAL becomes more and more important. To take into account these effects, we implemented a "parametric" method for low energy photons that uses the deposited energy and the energy centroid depth along the showed axis, evaluates the energy loss and adds all the contributions together. For higher energy, we found that a full three-dimensional fit of the shower energy deposition is more effective. This method is based on a precise modeling of the longitudinal and lateral development of shower inside the CAL. A reference axis needs to be known and is obtained from the tracker as it provides the best direction resolution. This method works for energies as high as $\sim$ 1 TeV (figure 3), above which the resolution degrades quickly because of crystal saturation and poor containment. A complete description of this algorithm and its performance can be found in [12].

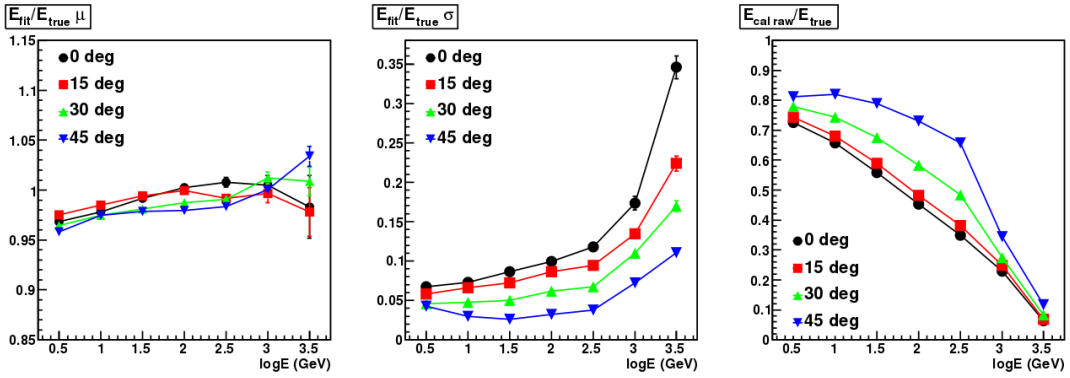

Figure 3: Performance of the shower profile fit (from [12]). (*left*) Bias. (*center*) Resolution. (*right*) Shower containment.

5. Future development

These years of nearly flawless operations allowed a constant improvement of the detector knowledge and, as a consequence, a periodic update of the events selection and corresponding instrument response parametrization. In parallel, the LAT team is working on a radical revision of the entire event-level analysis [13], based on experience gained in the prime phase of the mission.

One goal of this revision is recovering events contaiminated by instrumental pile-up effect (*ghost* signal, see [14] for more details). While only a few percent of the events are significantly affected by ghosts, the overal effect is a reduction of the efficiency that, in many cases can be recovered if we are able to identify and remove the spurious signal. Figure 4 shows an example of an event, a simulated gamma ray, is contaminated by ghost activity (from LAT periodic triggers).

The currect reconstruction is on the left where we can see that a small energy deposition far from the genuine event can flip the CAL axis. The result is a poor CAL–TRK matching and the event is discarded. To recover this class of events we introduced a clustering stage in the CAL, based on a Minimum Spanning Tree (MST) algorithm, that is capable to separate the genuine gamma-ray signal and provide topology information to the following reconstruction steps (right side of figure 4).

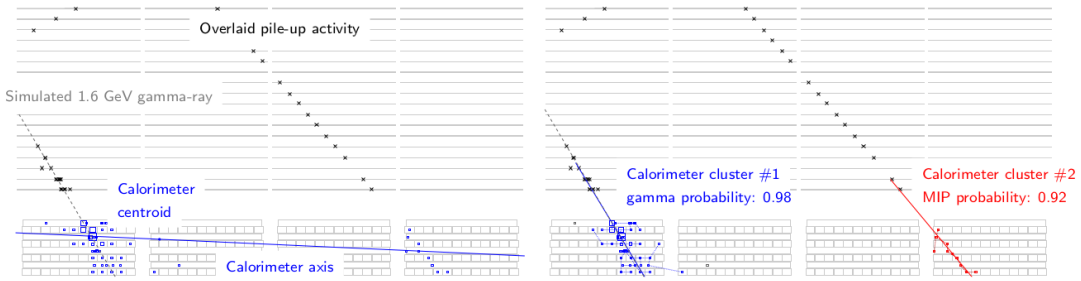

Figure 4: Effect of CAL clustering stage on event reconstruction. (*left*) Current reconstruction: we assume a single particle in the LAT. The CAL axis is flipped by ghost activity far from the gamma ray. (*right*) With CAL clustering: the gamma ray is isolated and the event is correctly reconstructed.

Another class of event that is currently discarded, and that we are trying to recover with a dedicated analysis are those with no usable TKR information. This can happen for gamma rays converting directly in the CAL or in case of mis-tracking due to large backsplash. We expect an increase of effective area at high energy. However, background rejection is more difficult for this events and real performance needs to be carefully evaluated.

6. Conclusions

The Fermi LAT has proven to be an excellent telescope for gamma rays above ~ 20 MeV. The LAT calorimeter works as designed with no major failures and no large performance variations. Thanks to its hodoscopic segmentation it provides a good energy resolution up to 300 GeV, still acceptable at 1 TeV and beyond, despite its modest depth. It also has good background rejection capabilities and good direction measurement ($\sim 2^\circ$ above 20 GeV). We are currently rewriting the reconstruction software to improve the instrument performance, taking into account the real data experience, including the extension of the energy reach up to 3 TeV. The Fermi LAT will continue to survey the sky and provide high-quality data for the whole physics community.

Acknowledgments

The *Fermi* LAT Collaboration acknowledges support from a number of agencies and institutes for both development and the operation of the LAT as well as scientific data analysis. These include NASA and DOE in the United States, CEA/Irfu and IN2P3/CNRS in France, ASI and INFN in Italy, MEXT, KEK, and JAXA in Japan, and the K. A. Wallenberg Foundation, the Swedish Research Council and the National Space Board in Sweden. Additional support from INAF in Italy and CNES in France for science analysis during the operations phase is also gratefully acknowledged.

References

[1] http://fermi.gsfc.nasa.gov/.

[2] P. L. Nolan et al. Fermi Large Area Telescope Second Source Catalog. *ApJS*, 199:31, April 2012. http://fermi.gsfc.nasa.gov/ssc/data/access/lat/2yr_catalog/.

[3] M. Ackermann et al. Fermi-LAT Observations of the Diffuse γ-Ray Emission: Implications for Cosmic Rays and the Interstellar Medium. *ApJ*, 750:3, May 2012.

[4] M. Ackermann et al. Constraining Dark Matter Models from a Combined Analysis of Milky Way Satellites with the Fermi Large Area Telescope. *PRL*, 107(24):241302, December 2011.

[5] M. Ackermann et al. Search for Gamma-ray Spectral Lines with the Fermi Large Area Telescope and Dark Matter Implications. *arXiv:1305.5597*, May 2013.

[6] M. Ackermann et al. Fermi LAT observations of cosmic-ray electrons from 7 GeV to 1 TeV. *PRD*, 82(9):092004, November 2010.

[7] M. Ackermann et al. Searches for cosmic-ray electron anisotropies with the Fermi Large Area Telescope. *PRD*, 82(9):092003, November 2010.

[8] W. B. Atwood et al. The Large Area Telescope on the Fermi Gamma-Ray Space Telescope Mission. *The Astrophysical Journal*, 697(2):1071, 2009.

[9] J. E. Grove and W. N. Johnson. The calorimeter of the Fermi Large Area Telescope. In *SPIE Conference Series*, volume 7732, July 2010.

[10] A. A. Abdo, , and et al. The on-orbit calibration of the Fermi Large Area Telescope. *Astroparticle Physics*, 32:193–219, October 2009.

[11] J. Bregeon, E. Charles, and M. Wood. Fermi-LAT data reprocessed with updated calibration constants. In *2012 Fermi Symposium proceedings - eConf C121028*, 2013. arXiv:1304.5456.

[12] Ph. Bruel. Gamma rays, electrons and positrons up to 3 TeV with the Fermi Gamma-ray Space Telescope. *Journal of Physics: Conference Series*, 404(1):012033, 2012.

[13] W. B. Atwood et al. Pass 8: Toward the Full Realization of the Fermi-LAT Scientific Potential. In *2012 Fermi Symposium proceedings - eConf C121028*, 2013. arXiv:1303.3514.

[14] M. Ackermann et al. The Fermi Large Area Telescope on Orbit: Event Classification, Instrument Response Functions, and Calibration. *ApJ Supplement*, 203:4, November 2012.